Nonnative Capping Structure Initiates Helix Folding in an Annexin I Fragment. A ^{1}H NMR Conformational Study

Benoît Odaert,[‡,§] Françoise Baleux,[||] Tam Huynh-Dinh,[||] Jean-Michel Neumann,[§] and Alain Sanson*[,§,⊥]

CEA, Département de Biologie Cellulaire et Moléculaire, SBPM, URA CNRS 1290, Centre d'Etudes de Saclay, 91191 Gif sur Yvette Cedex, France, and Unité de Chimie Organique, URA CNRS 487, Institut Pasteur, 28 rue du Dr Roux, 75724 Paris Cedex 15, France

Received April 26, 1995; Revised Manuscript Received July 26, 1995[⊗]

ABSTRACT: A 21-residue peptide, P_1AQFD$_5$ADELR$_{10}$AAMKG$_{15}$LGTDE$_{20}$D, corresponding to the (helix A)-loop motif of the second repeat of human annexin I, was synthesized and studied by 2D proton NMR. The conformational properties of the peptide were characterized at different temperatures in pure aqueous solution and in a TFE/H_2O (1:4 v/v) mixture. In pure aqueous solution, the peptide adopts a preferred conformation, comprising both elements of native and nonnative structures. A high α helix content is present in the DADELRA segment, which corresponds to an initiation site in the middle of the native α helix sequence. At the N-terminus flanking region, a particular nonnative folding is revealed by the J(NH−CHα) coupling constants and a set of unusual NOE connectivities which correspond to a helix interrupt at the first D residue. Addition of relatively small amount of TFE restores the native helix fold at the C-terminus but not at the N-terminus. On the contrary, the nonnative N-terminus structure is clearly stabilized by TFE. Our data indicate that this structure comprises (i) an Asp$_5$-x-x-Glu$_8$ N-terminal capping box, as recently named by Harper and Rose [Harper, E. T., & Rose, G. D. (1993) *Biochemistry 32*, 7605−7609], (ii) a (i,i+3) Asp$_7$-x-x-Arg$_{10}$ salt bridge, and (iii) a hydrophobic cluster centered on Phe$_4$ which mainly interacts with Leu$_9$ but also with Ala$_2$, Ala$_6$, and Ala$_{12}$ in a dynamic way. This structure is rather stable since it is still observed at 293 K in aqueous solution and 313 K in the presence of TFE. It constitutes a very potent initiation site of the α helix structure. This is, however, a nonnative structure involving highly conserved residues in the whole annexin family and thus may play an important role in the folding pathway as a transient "compacting helper".

Understanding how a polypeptide chain folds into a particular 3D structure remains a central interest in biochemistry not only from a fundamental standpoint but also from the more practical standpoint of protein engineering and design. Several experimental results (Chaffotte *et al.*, 1992; Jennings *et al.*, 1993; Dobson *et al.*, 1994; Hooke *et al.*, 1994) on protein folding revealed that secondary structures, especially α helix, are formed very early and probably within the first millisecond of the folding process. How such an efficient initiation of folding takes place and how it is related to the amino acid sequence is one of the main questions to be answered for understanding protein folding.

Protein fragments which have lost all or part of their long-range interactions normally leading to a cooperative folding can be used as pertinent indicators of the local early state of the protein folding (Wright *et al.*, 1988; Dyson *et al.*, 1992a,b; Waltho *et al.*, 1993; Schin *et al.*, 1993a,b; Zhou *et al.*, 1993; Shaw *et al.*, 1994; Pintar *et al.*, 1994; Muñoz & Serrano 1994, 1995). Fragments spanning elements of the secondary structure are important for understanding initiation, propagation, and stability of these structures. In addition, a step by step increase of the fragment length may help us to understand how long-range interactions take place to initiate the protein collapse into a compact state. We are currently using this approach to analyze folding and stability of a protein of the annexin family (Macquaire *et al.*, 1992, 1993). Annexins (Moss, 1992; Raynal & Pollard, 1994) constitute a new interesting protein model because of their highly hierarchical structure: four strongly homologous ≈70 residue domains assembled into two modules (Huber *et al.*, 1990a,b, 1992; Sopkova *et al.*, 1993; Weng *et al.*, 1993). Each domain is made of five helices, successively named A−F and folded into a characteristic superhelix motif: (A-loop-B)-C-(D-E).

We focused on domain 2 of human annexin 1 because it harbors the typical annexin Ca^{2+} site. Several fragments, ranging from 20 to 70 residues in length, thus spanning single helices up to the full domain 2, have been synthesized. Recently, we presented proton NMR[1] results on a 32-residue fragment spanning the A-loop-B segment (Macquaire *et al.*, 1993). This fragment was studied using three different environments: pure aqueous solutions, aqueous solutions containing small amounts of organic solvent (TFE), and aqueous solutions containing phospholipidic micelles (DPC). Whatever the environment, the A-helix was definitely found to be initiated at the first Asp residue in the sequence, that

‡ Present address: Institut Pasteur, SCBM, 1 Rue du Pr. Calmette, 59000 Lille, France.
§ SBPM, CNRS.
|| Institut Pasteur.
⊥ Also from Université P. et M. Curie, 9 Quai Saint-Bernard, Bât. C, 75005 Paris, France.
⊗ Abstract published in *Advance ACS Abstracts,* September 1, 1995.

[1] Abbreviations: DPC, dodecylphosphocholine; DG-SA, distance geometry-simulated annealing; EDTA, ethylenediaminetetraacetic acid; JR, jump and return pulse sequence; NMR, nuclear magnetic resonance; NOESY, nuclear Overhauser enhancement spectroscopy; TFE, trifluoroethanol; TOCSY, total correlated spectroscopy.

0006-2960/95/0434-12820$09.00/0

is, 4−5 residues downstream from the presupposed native helix start point. However, for fluorescence studies, a Phe→Trp mutation was introduced in the original sequence (AQ*W*DADEL... instead of AQ*F*DADEL...) which could induce a destabilization of the helix by strengthening the role of the following Asp residue, as a simple "helix stop signal" (Presta & Rose 1988). To address this problem and thus to examine the competence of particular sequences to initiate α-helix folding, a 21-residue fragment, the A-helix-loop motif, with the original sequence, P_1AQFD$_5$ADELR$_{10}$-AAMKG$_{15}$LGTDE$_{20}$D, was synthesized and studied by standard 2D proton NMR. Besides, the use of a shorter peptide minimizes the occurrence of resonance degeneracies often observed for partially folded helix fragments which may, in particular, obscure side-chain to main-chain as well as side-chain to side-chain contacts.

The present study demonstrates that the peptide adopts, in aqueous solution, a particular and significantly populated structure which initiates the helix at the first Asp residue. This initiation structure comprises (i) a capping box, D$_5$-x-x-E$_8$, whose structure displays a reciprocal side chain−main chain hydrogen bonding $i \leftrightarrow i+3$ network as it was recently emphasised (Harper & Rose, 1993), (ii) a D$_7$-x-x-R$_{10}$ salt bridge, and (iii) a set of hydrophobic interactions involving F$_4$ and L$_9$ as central residues but also A$_2$, A$_6$, and A$_{12}$. The thermal stability of this initiation structure, for two different solvent environments, was also examined. In aqueous solution the capping network was still present at 293 K. The stability even increased up to 313 K in a H_2O/TFE (4:1 v/v) mixture.

In the context of protein folding, this relatively high stability is of major importance. The **F-*D*-A-D-*E*-L-R** structural motif, located *near the middle* of the A-helix, is a nonnative structure, i.e., not maintained in the final protein organization where the two highly conserved ***D*** and ***E*** residues are involved in important salt bridges of the annexin tertiary structure. In addition, it is located near the hinge between module 1 (domains 1−4) and module 2 (domains 2−3). We postulate that this **F-*D*-A-D-*E*-L-R** stop (or start) signal could play an important *structural* and *kinetic* part in the protein folding pathway in the annexin family.

MATERIALS AND METHODS

Peptide Synthesis. The peptide was synthesized by the Merrifield (Merrifield, 1963) solid-phase method on an Applied Biosystem 430A synthesizer. The synthesis was performed using 0.5 mmol of Boc Asp(*o*-benzyl)Pam resin. Stepwise elongation of the peptide chain was done using the standard coupling-capping protocols.

The peptide resin (1.7 g) was subjected to the low-high HF cleavage (Tam & Heath, 1983). The crude peptide (356 mg) was purified on Bio-Gel P2 using 50 mM ammonium hydrogenocarbonate buffer, pH 6.8 (the peptide being more soluble in a basic buffer because of its high acidic amino acid content). The peptide (250 mg) was then purified on a Nucleosil 5 μm C18 300 Å semipreparative column, using a 10−50% linear gradient of acetonitrile in 50 mM ammonium acetate for 20 min at a 6 mL/min flow rate. The final purity of the peptide (99%) was checked on a Nucleosil 5 μm C18 300 Å analytical column, using a 17−37% linear gradient of the same eluents as above, at a 1 mL/min flow rate (retention time, 13.67). Yield: 40 mg. Positive ion electrospray ionization mass spectra: 2251.8 Da (expected: 2251.4 Da).

NMR Experiments. Samples were prepared from 5 mg of pure peptide dissolved in $^1H_2O/^2H_2O$ (90:10) 10 mM phosphate buffer containing 0.1 mM EDTA or in ^1H_2O/TFE (80:20) Tris buffer, to give a final concentration of 5 mM. The pH was adjusted to 4.5 in most experiments. A set of NOESY and TOCSY phase-sensitive spectra was collected either on a Bruker AMX 500 or on a Bruker AMX 600 spectrometer at different temperatures from 278 to 313 K. The water resonance was suppressed either by presaturation or by using the jump and return sequence (Plateau & Guéron, 1982). In general, 48 (TOCSY) or 80 (NOESY) transients were acquired with a recycling delay of 1 s. A total of 512 increments of 2K data points were collected for each 2D experiment yielding a digital resolution of 6 or 8 Hz/point in both dimensions after zero filling. Shifted squared sine-bell functions were used for apodization. The mixing time was 150 or 300 ms for NOESY experiments and 80 ms for TOCSY experiments. A NOE build-up curve was established with mixing times varying from 80 to 500 ms for the aqueous solution.

The absence of any aggregation effect on the peptide structure was assessed by recording a NOESY spectrum (300 ms mixing time) at 10 °C on a 10× diluted (0.5 mM) aqueous solution. The amide and α proton chemical shifts were found identical, within experimental errors, to those measured for the 5 mM solution, and the characteristic Nβ (5,8) NOE (see the result section) was observed with the same relative intensity.

Molecular Modeling. We used the last release, 6.1, of Sybyl (Tripos) which contains an efficient DG-SA subroutine. NOE constraints were classified according the four following ranges: strong (1.8−2.8 Å), medium (1.8−3.8 Å), weak (1.8−4.5 Å), and very weak (1.8−5.5 Å). In several calculations, the F4 side-chain constraints involved in the hydrophobic cluster were deliberately increased up to 6 Å to account for the intrinsic flexibility of the molecule. No hydrogen bonding constraints were introduced. Briefly, the molecule was first roughly energy minimized after embedding and submitted to equilibration at 800 or 1000 K for 2 ps followed by a cooling step to 0 K for 2.5 ps. High temperature equilibration and cooling steps were repeated several times. Tripos force fields were used with electrostatics. A final minimization was finally done. Structure predictions were performed using several algorithms: Garnier-Osguthorpe-Robson (GOR), Maxfield-Scheraga, Quian-Seynowski, and Holley-Karplus.

RESULTS

NMR Data of the Annexin I Fragment Solubilized in Pure Aqueous Solution. Figures 1 and 2 respectively show parts of the amide and aromatic regions respectively of the NOESY spectrum for the protein fragment solubilized in aqueous solution. The sequential assignment of the peptide resonances was achieved on the αN and the βN regions of TOCSY and NOESY spectra. The resonance assignment at 278 K is shown in Table 1. Figure 3 shows the complete set of characteristic NOEs observed at 278 K. The J(NH−CHα) coupling constants and the temperature coefficients of amide resonances are represented in Figure 5 and Table 3, respectively.

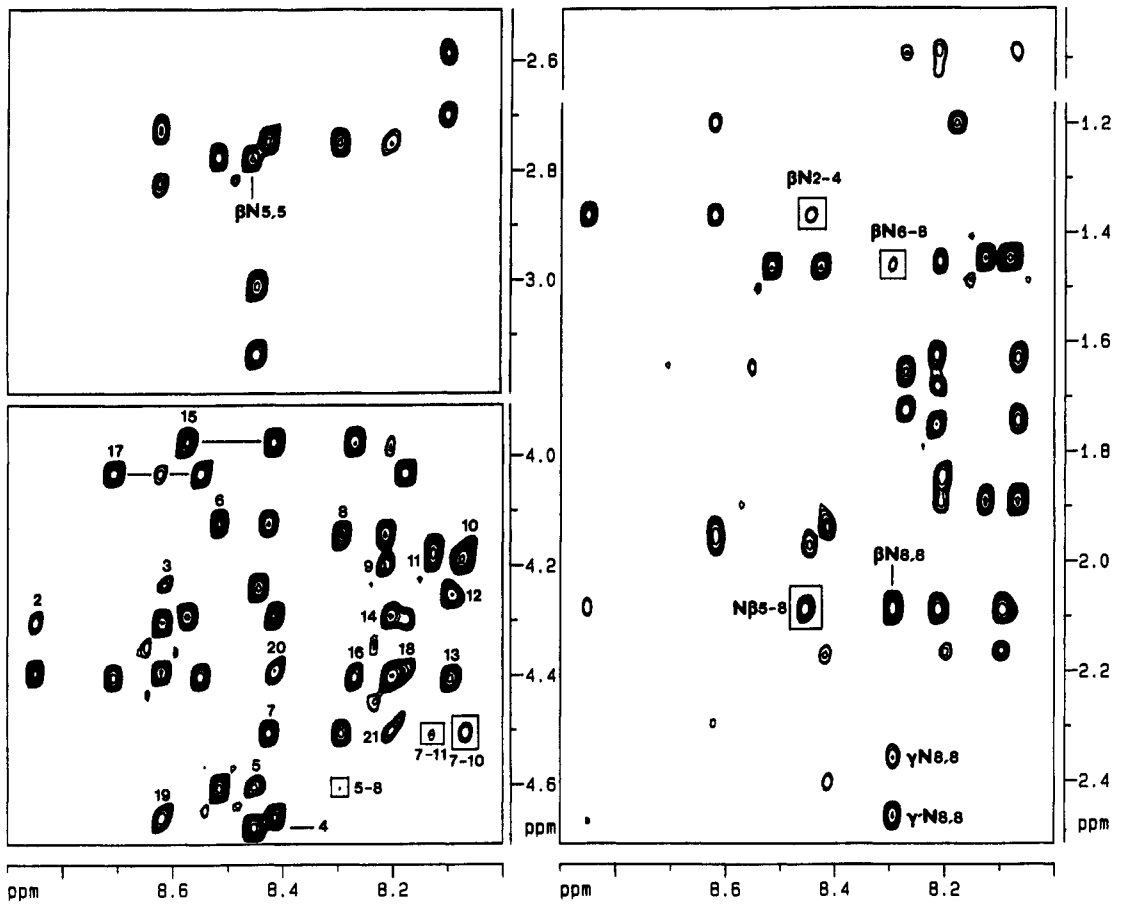

FIGURE 1: Amide region of the NOESY spectrum of the annexin fragment solubilized in the aqueous solution at pH 4.5, $T = 278$ K. The αN(5,8) cross-peak is unambiguously detected in maps drawn at lower level.

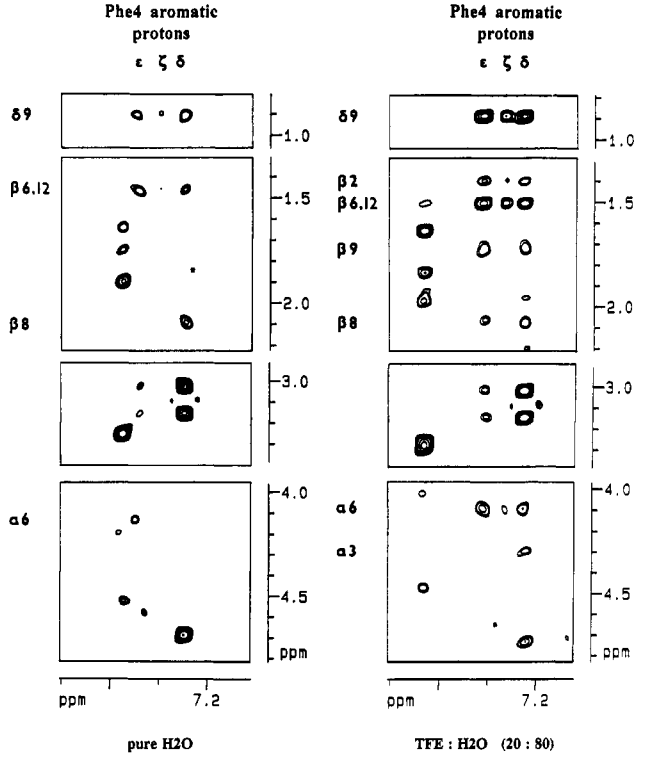

FIGURE 2: Aromatic region of the NOESY spectrum of the peptide, in aqueous solution at pH 4.5, $T = 278$ K (left) and in a TFE/H2O mixture (20:80 v/v, pH ~4.5, 278 K) (right).

From the NOE pattern, three different regions of the peptide can be delimited. A central region A6−A11 for which a nearly complete set of medium range (i,i+3) NOE connectivities indicates a local stable α helix conformation. The two flanking regions do not seem to adopt a particular folded conformation as suggested by the strength of the αN(i,i+1) NOE connectivities and the reduced intensity or the absence of NN(i,i+1) or βN(i,i+1) NOE connectivities.

As regards the central region, the strong NN(i,i+1) NOEs associated with the medium αN(i,i+1) NOEs reveal a backbone preference for α helix structure. Very small NN(i,i+2) are also observed indicating a rather strong compactness of the structure in this region. A complete set of αβ(i,i+3) NOE connectivities and the presence of the αN(7,10) and αN(7,11) NOEs also argue for a high population of α helical structure in the A6−A11 segment. Unfortunately, the numerous overlaps within the proton signals of the C-terminus flanking region prevent us from assessing whether the α helix propagates up to K14−G15 which are the native C-terminal residues of the helix A. However, the relatively low temperature coefficients of the R10 to M13 amide resonances (~−4 ppb/K) and the small values (Figure 5) of the corresponding J(NH−CHα) coupling constants confirm the previous results and suggest that the helix structure tends to propagate one additional turn toward the C-terminus. The α proton chemical shift curve of Figure 6 also supports this view. Indeed, when dealing with conformational equilibrium, chemical shift data become important as folding reporters because they are statistical average values over *all the configurations* experienced by the peptide when NOEs represent statistical average values over only a more limited number of configurations, those with interproton distances approximately smaller than 5 Å and sufficiently

Table 1: ^{1}H Chemical Shifts of the Peptide in Aqueous Solutions at 278 K, pH 4.5

	NH	αH	βH	others			
P1		4.41	2.49/2.07	γCH$_2$	2.04/1.19	δCH$_2$	3.67/3.41
A2	8.86	4.31	1.37				
Q3	8.63	4.25	1.95/1.95	γCH$_2$	2.30/2.22	NH$_2$	7.68/6.99
F4	8.45	4.69	3.15/3.02	δ 7.25		ϵ 7.35	ζ 7.30
D5	8.46	4.62	2.78/2.78				
A6	8.52	4.13	1.46				
D7	8.43	4.41	2.75/2.75				
E8	8.30	4.15	2.09/2.09	γCH$_2$	2.47/2.36		
L9	8.21	4.20	1.75/1.75	γCH$_2$	1.62	δCH$_3$	0.93/0.89
R10	8.06	4.17	1.89/1.89	γCH$_2$, ϵNH	1.74/1.62, 7.38	δCH$_2$, ηNH$_2$	3.25, 6.99/6.56
A11	8.13	4.19	1.44				
A12	8.09	4.26	1.44				
M13	8.10	4.41	2.09/2.09	γCH$_2$	2.70/2.60	ϵCH$_3$	2.16
K$_{14}$	8.20	4.30	1.89/1.84	γCH$_2$, ϵCH$_2$	1.45, 3.00	δCH$_2$, ζNH$_3$	1.68, 7.65
G15[a]	8.42/8.58	3.97					
L16	8.27	4.41	1.72/1.72	γCH	1.65	δCH$_3$	0.95/0.89
G17[a]	8.55/8.71	4.03					
T18	8.18	4.40	4.30/4.30	γCH$_3$	1.20		
D19	8.63	4.67	2.83/2.73				
E20	8.42	4.40	1.94/1.94	γCH$_2$	2.41/2.17		
D21	8.20	4.50	2.81/2.75				

[a] G15 and G17 are ^{15}N-labeled.

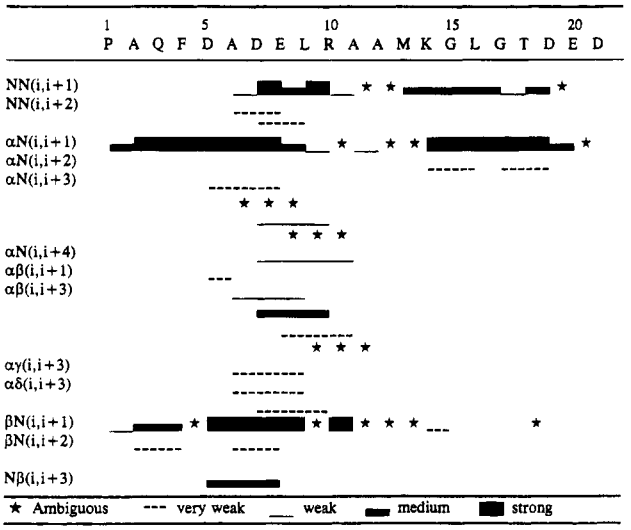

FIGURE 3: Diagram showing the ensemble of NOE connectivities within the Annexin fragment in aqueous solution at pH 4.5, T = 278 K.

long life time. As a consequence, the chemical shift difference $\Delta\delta_\alpha = \delta_{obs} - \delta_{coil}$ for the α protons may be considered as a folding index (Wishart *et al.*, 1991, 1992). δ_{obs} is the experimental H_α chemical shift and δ_{coil} is the corresponding coil value as given by Merutka *et al.* (1995). In the 6−13 region $\Delta\delta\alpha$ exhibits negative values and draws a (i,i+4) oscillation characteristic, though smooth, of a α helical structure (Jiménez *et al.*, 1992; Blanco *et al.*, 1992), followed by a progressive return to the random coil values. The presence of a (i,i+3) D7−R10 salt bridge is supported by the presence of very weak connectivities between D7 and R10 protons: αδ(7,10), αNϵ(7,10), and βN(7,10). The low thermal coefficient of the ϵ amide proton of the R10 side chain, −3.5 ppb/K, suggests a hydrogen-bonding with the γ carboxylate of the D7 side chain. However, the magnetic equivalence of the β protons of both side chains indicates a relative flexibility in this salt bridge.

As regards the 14−21 C-terminus segment, the presence of medium NN(i,i+1) and strong αN(i,i+1) NOEs is characteristic of an interconversion between different conformations. A small population of β turn-like structures is also revealed by the presence of very weak (i,i+2) contacts (Figure 3).

Table 2: NOE Connectivities in the Capping Structure (5 °C)[a]

NOE	H$_2$O	H$_2$O/TFE
Capping Structure		
αα(5,6)	vw	w
αβ(5,6)	vw	m
ββ(5,6)		vw
ββ(5,8)	vw	vw
Nβ(5,8)	m	★ (§)
Nβ(5,9)		vw
Nγ(5,9)		w (§)
Nδ(5,9)		vw
βα(6,7)		m
ββ(6,7)		vw
βN(6,8)	vw	w (§)
γN(8,9)		vw
Hydrophobic Cluster Interactions		
βδ(2,9)		vw
βN(2,4)	vw	m
ββ(4,8)		vw
βδ(4,9)	vw	m
β{δ,ϵ,ζ}(2,4)		w
α{δ,−,−}(3,4)		w
{δ,ϵ,−}N(4,5)		vw
{δ,ϵ,−}β(4,8)	w	vw
{−,ϵ,−}N(4,9)		vw
{δ,ϵ,−}β(4,9)		w
[δ,ϵ,ζ]γ(4,9)		m (#)
{δ,ϵ,ζ}δ(4,9)	w	m
{δ,ϵ,−}N(4,12)		vw
[δ,ϵ,ζ]β(4,12)	w (#)	m (#)
{δ,ϵ,ζ}α(4,6)	vw	vw
[δ,ϵ,ζ]β(4,6)	w (#)	m (#)

[a] NOE intensities: m, medium; w, weak; vw, very weak. ★, ambiguous at 5 °C, w at 40 °C. (§) resolved at pH 6.4. (#) mutually ambiguous. { } = "and" [ ] = "or".

As regards the N-terminus flanking region of the α helical region, the lack of NN(i,i+1) NOEs and the strength of the αN(i,i+1) NOE connectivities do not suggest any folded conformation. However, numerous unusual NOE connectivities are observed (Figure 1 and Table 2) and, most noteworthy, a characteristic Nβ(5,8) NOE, suggesting a local

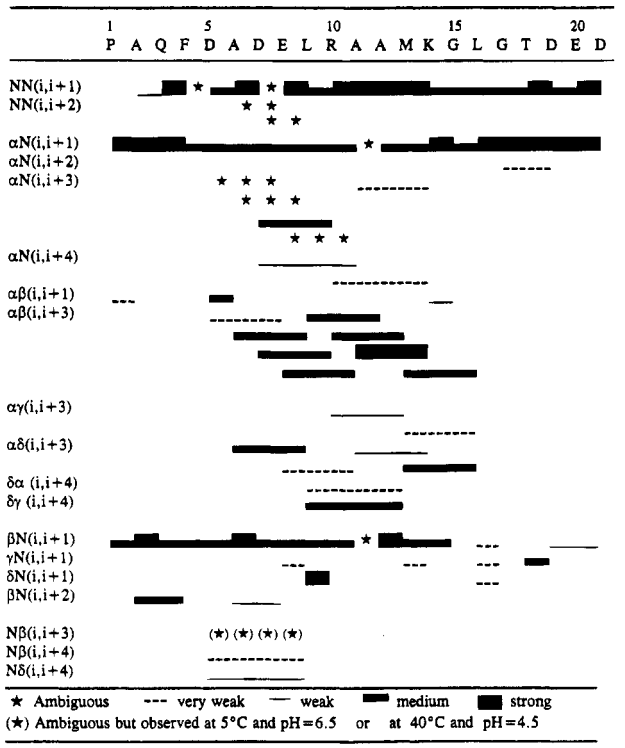

FIGURE 4: Diagram showing the ensemble of NOE connectivities within the annexin fragment in TFE/ H2O mixture (20:80 v/v, pH ~4.5, 278 K).

Table 3: Temperature Coefficients of the Amide Proton in Aqueous Solution and H_2O/TFE (ppb/K)

residue	H_2O	H_2O/TFE
P1		
A2	−6.5	−7
Q3	−9.5	−10
F4	−8.5	−7
D5	−6	−5.2
A6	−8.5	−9
D7	−5	−3
E8	−4.2	−4
L9	−6.5	−6.5
R10	−4	−6.5
A11	−4.6	−3
A12	−3.8	−5.2
M13	−3.2	−5
K14	−5	−2.8
G15	−5.5	−3
L16	−6	−3
G17	−6	−5.5
T18	−6.5	−5.5
D19	−7	−6
E20	−7	−6
D21	−6	

folding back of the N-terminal part of the peptide backbone at the initiation point of the α helix structure. Such a folding is confirmed by the numerous NOE contacts observed between the side-chain protons of F4 and L9 residues characteristic of the presence of a hydrophobic cluster (Figure 2 and Table 2). Lastly, the high value of the D5 J(NH−CHα) coupling constant (7.5 Hz), as compared to that of the following residue (4 Hz), shows that D5 is the transition residue between the N-terminus and the beginning of the helix structure. This set of results is consistent with a local structure now described (Harper & Rose, 1993; Lyu *et al.*, 1993, 1994) as an N-capping box and showing a reciprocal

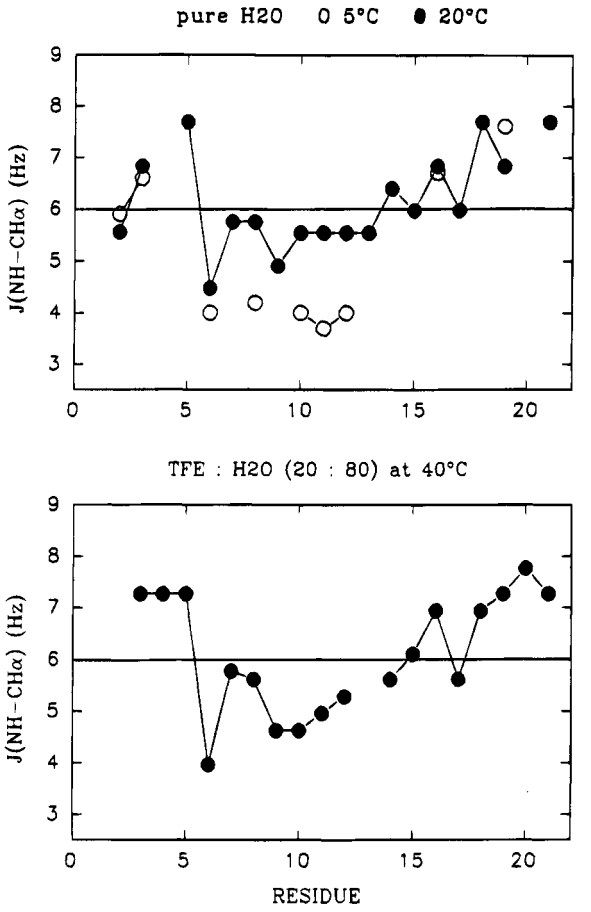

FIGURE 5: J(NH−CHα) coupling constants in the annexin fragment: aqueous solution, pH 4.5, T = 278 K (○) or T = 313 K (●) (top) and TFE/ H_2O mixture (20:80 v/v, pH ~4.5) at T = 313 K (bottom).

backbone to side-chain hydrogen-bonding interaction between the N-cap residue (D5) and the N+3 residue (E8). However, the thermal coefficient of the D7 amide proton (Table 3), although typically smaller than random-coil values (Merutka *et al.*, 1995), is higher than one would expect for a strong hydrogen bond. The capping-box structure is most likely in exchange with other conformations.

Considering the potential importance of the D5−E8 capping box in the folding process, we decided to assess its stability by varying either the temperature or the solvent. We first tested the ability of an organic solvent (TFE) to destabilize the capping structure by disrupting the hydrophobic cluster described above.

NMR Data of the Annexin I Fragment Solubilized in TFE/ H_2O Mixture. The complete assignment in TFE/ H_2O mixture (20:80 v/v, 278 K) is listed in Table 4. NOE connectivities and thermal coefficients of amide resonances are presented in Figure 4 and Table 3, respectively. The J(NH−CHα) coupling constants at higher temperature, 313 K, are also shown in Figure 5, and lastly the chemical shift variation of the α protons are shown in Figure 6.

As expected, a full set of $\alpha\beta(i,i+3)$ NOE connectivities is observed upon addition of TFE demonstrating the stabilization of the α helix which now extends up to L16 (Figure 4). This is confirmed by the upfield shift and the characteristic sharp oscillations of the corresponding α proton resonances (Figure 6), the low values of the J(NH−CHα) coupling constants (only shown at 313 K, Figure 5), and the

Table 4: ^{1}H Chemical Shifts of the Peptide in H_2O/TFE (80:20 v/v) at 278 K, pH 4.5

	NH	αH	βH	others			
P1		4.39	2.47/2.06	γCH$_2$		δCH$_2$	3.40
A2	8.84	4.31	1.36				
Q3	8.55	4.26	1.99/1.94	γCH$_2$	2.29/2.24	NH$_2$	7.64/6.87
F4	8.22	4.71	3.12/2.99	Hδ 7.20		Hε 7.35	Hζ 7.24
D5	8.25	4.67	2.79/2.86				
A6	8.58	4.05	1.47				
D7	8.32	4.45	2.80/2.70				
E8	8.24	4.08	2.17/2.06		2.52/2.36		
L9	8.09	4.09	1.70/1.70	γCH	1.48	δCH$_3$	0.86/0.86
R10	8.16	4.00	1.94/1.89	γCH$_2$, εNH	1.80/1.61, 7.40	δCH$_2$, ηNH$_2$	3.26/3.22, 6.90/6.50
A11	7.91	4.13	1.48				
A12	8.08	4.17	1.47				
M13	8.14	4.27	2.13/2.13	γCH$_2$	2.73/2.53	εCH$_3$	2.03
K14	7.95	4.21	1.91/1.91	γCH$_2$, εCH$_2$	1.56/1.46, 2.99	δCH$_2$, ζNH$_3^+$	1.72, 7.68
G15[a]	8.18/8.34	3.97					
L16	7.98	4.39	1.76/1.76	γCH	1.63	δCH$_3$	0.94/0.89
G17[a]	8.32/8.48	4.03					
T18	8.09	4.40	4.28/4.28	γCH$_3$	1.20		
D19	8.56	4.67	2.83/2.73				
E20	8.36	4.40	1.94/1.94	γCH$_2$	2.41/2.17		
D21	8.13	4.51	2.83/2.77				

[a] G15 and G17 are ^{15}N-labeled.

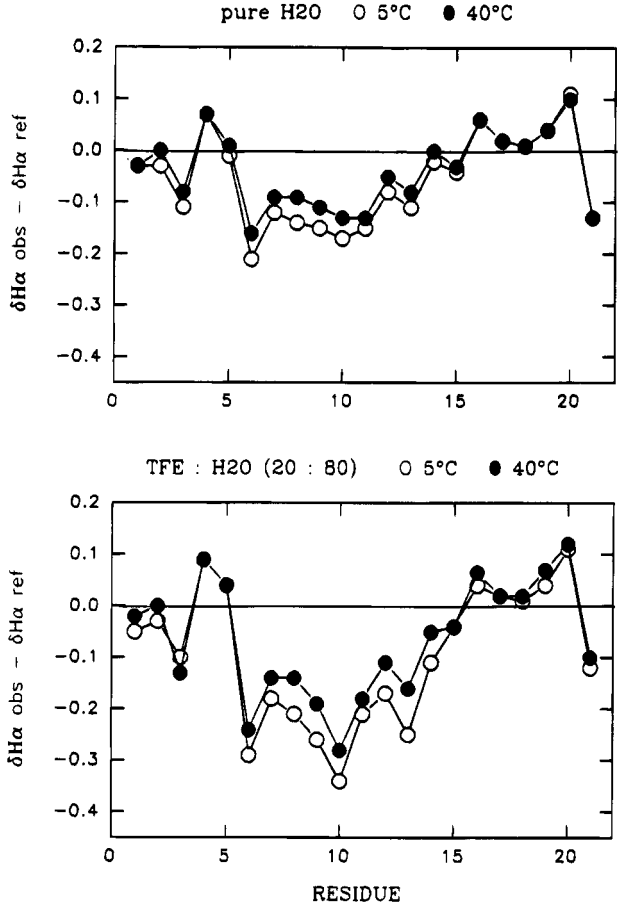

FIGURE 6: α Proton chemical shift differences $\Delta\delta_\alpha = \delta_{obs} - \delta_{coil}$ for the two solvent conditions: aqueous solution, pH 4.5 (top) and TFE/ H_2O mixture (20:80 v/v, pH ~4.5) (bottom) and for two different temperatures, T = 278 K (O) and T = 313 K (●).

lowering of the amide proton thermal coefficients (Table 3). Lastly, the D7−R10 salt bridge is clearly stabilized as suggested by the magnetic inequivalence of the β protons and the increased intensity of the αδ(7,10), αNε(7,10) NOEs and the presence of very weak Nεβ(10,11), Nηβ(10,11) NOEs and the intraresidue NNη(10,10) NOE.

While the α helix propagation occurs toward the C-terminus, no indication of such a process for the N-terminus is found. The nonnative capping structure observed in water is even clearly stabilized by the addition of TFE.

First, the increase in the number and intensity of the NOE cross-peaks between the aromatic protons of F4 and the backbone as well as the side-chain protons of residues A2 and L9 but also A6 and A12 (Figure 2 and Table 2) indicate stronger packing of the local hydrophobic cluster than when it was observed in water. A very weak contact between βA2 and δL9 protons is also detected. Second, the increase in intensity of the NOE cross-peaks previously observed in water and the presence of additional NOE connectivities like Nβ(5,9) (Table 2) confirm the stabilization of the N-capping structure. Because of signal overlaps, the characteristic Nβ-(5,8) NOE was not unambiguously detected under the initial experimental conditions; however, this NOE was clearly observed by simply increasing either the pH, from 4.5 to 6.4 (data not shown), or the temperature, to 313 K. A weak Nδ(5,9) contact and a very weak Nβ(5,9) contact are also observed and confirm the folding back of the Asp5 amide proton.

NOE data relative to the hydrophobic cluster deserve additional analysis. Indeed, a survey of Table 2 shows that the ensemble of NOE contacts between Phe4 side chain and the other residues are likely to represent several conformations rather than a unique conformation. In the context of an α helix starting at residue D5, it is difficult, for instance, to insert simultaneously the A5−F4 and F4−E8/L9 interactions into a single conformation. The ensemble of peptide configurations is better represented by the F4 side chain fluctuating inside a "near hydrophobic pocket" made on one hand by A2 and probably the nearby Q3 side-chain methylenes and, on the other hand, by the hydrophobic residues running from A6 to A12. This dynamic picture of the hydrophobic cluster is qualitatively emphasized in Figure 7B showing different structures of the P1−G15 part of the peptide obtained by DG-SA, starting from different restricted sets of acceptable NOE constraints between the F4 side chain and the other hydrophobic side chains. Such a conforma-

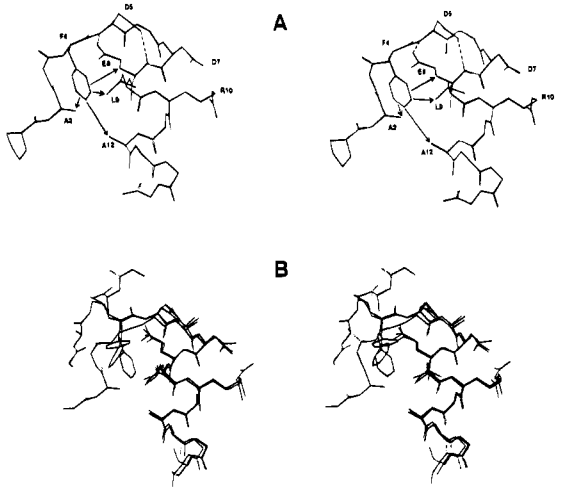

FIGURE 7: Peptide structure derived from NOE data observed for the TFE/ H_2O solution. (A) A model of the P1−G15 part of the peptide satisfying most of the NOE constraints involving the F4 protons. (B) Superposition of three structures satisfying three different sets of NOE constraints for the F4 protons.

tional exchange may be associated with transient breaking of the main-chain to side-chain D5−E8 hydrogen bond. Figure 7A shows one probable configuration compatible with the maximum number of experimental NOEs, those excluding F4−A6 interactions and thus favoring the capping box hydrogen-bonded structure. Of course these calculations *do not intend* to properly describe the dynamic aspects of the conformational fluctuations of the peptide. Only thorough molecular dynamics on the solvated peptide will be able to give a correct picture. This is the object of another work.

Finally we observe that, suprisingly, the TFE did not disrupt the hydrophobic cluster but, on the contrary, increased its stability by reinforcing the hydrogen-bonding network of the capping structure. This effect was already observed in other peptide studies (Zaima *et al.*, 1993; Wray *et al.*, 1994; Smith *et al.*, 1994).

Thermal Stability of the Capping Structure. The thermal stability of the N-terminal capping structure was studied for both solvents by recording NOESY maps at several temperatures ranging from 278 to 313 K. In order to appreciate the thermal stability of the capping structure, we used the three complementary indexes: (i) the qualitative intensities of some characteristic NOE contacts, namely, NN(i,i+1), $\alpha\beta$-(i,i+3), and Nβ(i,i+3) (data not shown), (ii) the α proton chemical shifts (Figure 6), and (iii) the J(NH−CHα) coupling constants (Figure 5).

First we observe, over the 35 K temperature range, that the ensemble of NMR data do not exhibit any sharp or cooperative variation but a rather small and smooth variation. From the NOE standpoint, which is the most demanding as concerns time scale and structural coherence, the capping structure and helix propagation are clearly maintained above 293 K for the aqueous solution and above 313 K for the H_2O/TFE solution. Indeed, for the aqueous solution, the $\alpha\beta$-(6,9), the $\alpha\beta$(7,10), and the Nβ(5,8) NOEs are still observed at 293 K, and, for the 20% TFE solution, six $\alpha\beta$(i,i+3) distributed over the segment D5−K14 and the Nβ(5,8) NOEs are still observed at 313 K. In terms of NOEs and J(NH−CHα) coupling constants, the addition of 20% TFE increases the general stability of the conformations observed in water by at least 35 K.

As already stated chemical shifts and coupling constants are statistical averages over the whole conformational space explored by the peptide. In this respect, both the values of chemical shifts and coupling constants obtained for the H_2O/TFE solution indicate that the A6−M13 peptide segment still possesses a relatively important helix statistical weight at 313 K. Assuming that the state of this segment at 278 K is 100% helix and that the relationship between $\Delta\delta_\alpha$ and helix weight is linear, the helix weight would still remain above 80% at 313 K.

For the aqueous solution, the J(NH−CHα) coupling constants in the A6−M13 peptide segment are close to the coil values when $T \geq 293$ K although they do not exceed 6 Hz. On another hand, the chemical shift values remain definitely within the α helix values, even at 313 K. The apparent discrepancy can be explained as follows:

(i) J(NH−CHα) coupling constants only depend on the backbone φ dihedral angle fluctuations. If one assumes that φ explores the whole accessible range of values observed *in the helix segments of proteins* [see, for instance, Oldfield and Hubbard (1994)], that is, $-45° \leq \varphi \leq -100°$, then J is allowed to range between ~3 and ~9 Hz, giving an average of ~6 Hz. Our experimental values clearly remain close to this value at the high temperatures explored.

(ii) The chemical shift index $\Delta\delta_\alpha$ will change from strictly negative (α helix) to strictly positive (β sheet) values if, respectively, the backbone angle ψ changes from the [−60°,+10°] range to the [110°, 165°] range (Oldfield & Hubbard, 1994) and if φ predominantly explores the [−90°,−150°] range. Only very large amplitude fluctuations of the ψ dihedral angle and thus exchange between the α and β regions of the Ramachandran plot will give small or zero values for $\Delta\delta_\alpha$. We therefore conclude that, in aqueous solution, even at 313 K, the A6−M13 segment of the peptide remains in the α helix conformational region for both φ and ψ dihedral angles.

DISCUSSION

The FDxxEL Motif as a Canonical N-Terminal Capping Structure. Since the initial observation of the capping-box structure (Lyu *et al.*, 1993), several protein sequences have been shown to code for a structure stabilizing α helices N-terminus and entering the framework of the capping-box model involving reciprocal side-chain−main-chain hydrogen bonding between the Ncap and N+3 residue (Lyu *et al.*, 1993; Harper & Rose, 1993; Seale *et al.*, 1994). Recently, an extended definition of the capping-box has been proposed which includes two flanking hydrophobic residues Ncap -1 and Ncap+4 (Seale *et al.*, 1994). The annexin FDxxEL sequence obviously fits this definition as revealed by the numerous interactions observed between the hydrophobic residues. A recent identical result, concerning a designed peptide involving the sequence FSxxEL, was also independently obtained (Muñoz *et al.* 1995). However, the DxxE capping pair is, to our knowledge (Seale *et al.*, 1994; Harper & Rose, 1993), one of the less frequent pairs as compared for instance to SxxE. If the frequency difference stands on stability difference, then there are two possible reasons for this: (i) the additional unfavorable electrostatic interaction between the D and E side-chain negative charges brought in close proximity in the capping structure and (ii) the additional bond involved in the Asp (or Asn) N-capping as

compared to Ser (or Thr) capping, which might confer to the helix N-terminus a slightly less compact structure than that provided by Ser capping. This is probably reflected in the φ and ψ dihedral angle distribution which is quite different for the two pairs of N-capping residues (Dasgupta & Bell 1993). The most recent estimation of the capping box energetics (Muñoz & Serrano 1995) does not, however, indicate difference between the SxxE and the DxxE capping boxes.

In our study, the DxxE stability is monitored by the thermal variations of the α proton chemical shifts, the αNH coupling constants, NOEs, and the thermal coefficients of the amide protons. On one hand, the existence of a detectable amount of structure at high temperature indicates a relatively high stability. On the other hand, the thermal coefficients of the D and E amide protons are higher than expected for a strongly hydrogen-bonded structure. Indeed, lower values were observed for a SxxE capping box (Jiménez *et al.*, 1994). Obviously the thermal coefficients data for D5 and E8 contain a temperature-dependent contribution of conformational exchange, through a modulation of the chemical shift. This reflects the existence, in our peptide and in addition to the main capping structure, of short-lived multiple configurations which are very likely associated with the hydrophobic cluster fluctuations. A better description and understanding of these aspects is expected from the analysis of the intensive molecular dynamics calculations we are performing and from the study of selectively mutated peptides.

The FDxxEL Motif as a Nonnative Structure in the Protein Folding Context. There is now a wide body of evidence that denatured or unfolded proteins as well as protein fragments are in a much less random state than initially thought. Alternatively they possess several kinds of residual structures generally reminiscent of the native structure. This aspect of protein folding has been reviewed by several authors (Montelione & Sheraga, 1989; Dill & Shortle, 1991; Dobson, 1992; Shortle, 1993). Protein fragments which have been shown to exhibit residual structure in aqueous solution are, up to now, essentially α helix segments of proteins. This is mainly because the hydrogen bond network is short-ranged in α helix as compared to β sheet. It is, however, out of the scope of this paper to review the whole work done in this field. Several results concerning turns as residual structures, which are important elements of secondary structure in the context of the protein folding process, have been also recently published (Zaima *et al.*, 1993; Wray *et al.*, 1994; Smith *et al.*, 1994; Zhang & Forman-Kay, 1995).

As concerns residual helix structure, the general picture which now emerges, mainly originating from several pioneering works (Wright *et al.*, 1988; Dyson & Wright, 1991; Dyson *et al.*, 1992a,b; Waltho *et al.*, 1993; Schin *et al.*, 1993a,b), is that the folding of small α helical globular proteins is initiated, at the very early stage, by helical embryos of various length. The length of these initiation structures varies from the most rudimentary "nascent helical structure" (Dyson *et al.*, 1992) to structures which contain a large population of well characterized helix motifs. However, nascent helices and single α helix turns are more common than stable α helices. In addition, these incomplete helices or "near helices" in aqueous solution are easily fully stabilized when a small amount of organic solvent (TFE) is added. The A-helix of annexin I domain 2 is one of those fragments exhibiting a high helix content at least in the C-terminal part beginning at the initiation site D5xxE8. However, this helix initiation site shows some particularities which make it a remarkable and well defined *nonnative structure* that must be further discussed.

First of all we observe that the DxxE motif initiates helix folding in the middle of the native A-helix of annexin I domain 2. It allows helix propagation toward the C-terminus but stops such a process toward the N-terminus by forcing the peptide backbone to fold back. From this standpoint the initiation site creates a strongly persistent *nonnative structure* in the A-helix. The D5−E8 hydrogen bond network is stabilized by an hydrophobic cluster mainly involving F4 and L9 residues and by the D7−R10 salt bridge. The salt bridge and the hydrophobic cluster behave as complementary nonnative structures. It is worth noting that hydrophobic clusters are likely to be important local residual features present during the early events of protein folding. Indeed native as well as nonnative hydrophobic clusters have been observed in protein fragments and unfolded proteins by several authors (Garvey *et al.*, 1989; Evans *et al.*, 1991; Broadhurst *et al.*, 1991; Neri *et al.*, 1992; Alexandrescu *et al.*, 1993; Smith *et al.*, 1994; Lumb & Kim, 1994) and by us (Macquaire *et al.*, 1993; Beswick *et al.*, unpublished results). These clusters seem to involve most exclusively one or several aromatic side chains, but it is not clear whether this simply results from the fact that they are easily detected because aromatic protons give rise to rather well separated NOE cross-peaks or whether this reflects more profound reasons. As concerns our peptide, the observed hydrophobic cluster is the result of the main chain reversal due to the capping structure but does not form independently, as judged by mutational analysis (Guerois *et al.*, work in progress). However, its participation in a larger transient hydrophobic cluster, during the initial collapse of the folding protein, cannot be excluded. From a more general standpoint, the role and the importance of these hydrophobic clusters in the folding process is not yet clearly elucidated. Probably they participate to the general trend of an unfolded protein to acquire compact structures involving local as well as long-range interactions during the initial period of the folding.

The second observation concerns the conservation, in the whole annexin family, of the residues involved in the nonnative structure and their structural fate in the final native state. Most of these residues are highly conserved in the domain 2 of every member of the annexin family [see, for instance, Raynal and Pollard (1994)] with the following "consensus" sequence: (F/Y)DAp(E/Q)L(R/K), where p is any polar amino acid. Remarkably, all the residues involved in the *local interactions* stabilizing the nonnative structure in the unfolded state are to be involved in important *nonlocal or long-range interactions* in the native folded state. This is depicted in Figure 8: in the native state, residue D5 makes a well conserved (i,i+25) salt-bridge linking the A and B helices and residue E8 also makes a conserved salt bridge linking domain 2 to domain 4. This local to nonlocal switching in the interactions involving the FDADELR segment can be rationalized: in the absence of the long-range interactions, the nonnative capping box present in the unfolded protein would be more stable than the full helix in the folded native state. Thus the long-range intra- and interdomain interactions not only stabilize the tertiary structure of the protein but also allow the nonnative structure

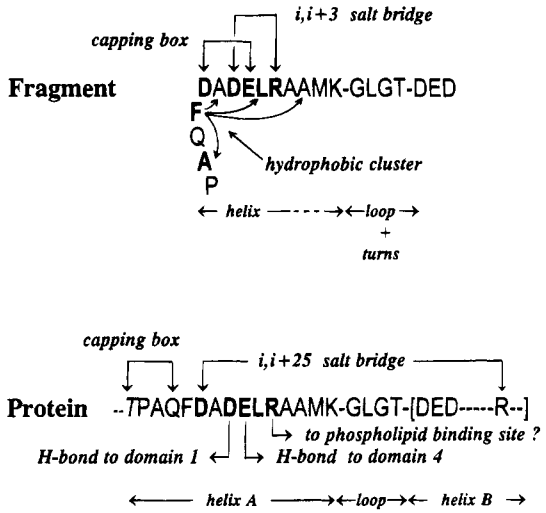

FIGURE 8: Schematic representation of the conformation and interactions in the annexin fragment (top) as compared to the conformation and interactions for the same segment in the native protein structure (bottom).

present in the unfolded state to be dismantled. Conformational switching within a protein segment and a high conservation of the involved residues in the protein family may serve to define and detect *sequence-encoded* folding determinants.

A third and complementary observation concerns the helix propensity of the N-terminal segment of the A-helix, upstream the DxxE sequence, to form a stable structure. Indeed, the published predictions (Taylor & Geisow 1987) as well as those we performed (see Materials and Methods) generally gave a low helix propensity for the N-terminal segment and a high propensity for the remaining part of the A-helix. The only exception comes from the GOR algorithm which predicts the correct native helix extension. The other methods seem better to predict the helix propensity of the fragment rather than the native helix extension. This would suggest the existence of a structural weakness in the N-terminal segment as opposed the high stability of DxxELR segment in the middle of the native A-helix. However, there are two exceptions, the annexin I and II where the A-helix N-terminal sequence is TPxQ which is typically a capping box consensus sequence. This capping box is indeed observed in annexin I (S. H. Kim, private communication). In this particular case, the existence of two sequential, thus competitive, capping boxes in the same helix remains a rather unexpected but interesting situation that we are presently studying.

What could be the role of the nonnative structure in the folding process in the annexin family? Considering the preceding ingredients, we may now hypothesize that, during the early stage of the folding, the nonnative (F/Y)Dxx(E/Q)L capping structure will predominantly form (at the expense of, or in parallel to, the TPAQ capping structure in the particular case of annexin I and II). As a consequence, a transient chain reversal will be formed, reducing the local conformational freedom and, more importantly, increasing the local protein compactness and thus enhancing the initial collapse. The nonnative structure will be removed at the final stage of folding when the side chains of residues D and E will be able to reorganize to form the native long-range salt-bridge interactions. It is also noteworthy that the FDxxEL structure is located near the hinge between domain 1 and domain 2, which are very weakly interacting domains in the final native structure.

From a more general standpoint, it is worth remembering that, in a protein segment having a high helix propensity, helix structure tends to form very rapidly, probably in a time scale shorter than 1 μs, thus creating somewhat of a rigid segment. Existence of nonnative, as well as native, local "compacting structures" may be necessary for the protein to reach a folding-competent 3D compact structure. As opposed to loops which *allow but not necessarily favor* compact structure formation, sufficiently persistent nonnative structures, as the one described in the present work, may play a crucial role by limiting the conformational space of the folding protein. This may even be considerably more important for large α helical proteins, like annexins, than for small proteins like those usually studied. Alternatively, these structures could, *in vivo*, optimize the cotranslational folding in another way, for instance by maintaining a sufficiently high level of compactness within the newly synthesized N-terminal part of the protein. This "continuous compacting" process could have some sort of an autochaperon effect during peptide elongation also limiting the formation of misfolded intermediates. We are now studying a series of annexin fragments selected for a better understanding of these aspects of protein folding.

REFERENCES

Alexandrescu, A. T., Evans, P. A., Pitkeathly, M., Baum, J., & Dobson, C. M. (1993) *Biochemistry 32*, 1707−1718.
Blanco, F. J., Herranz, J., Gonzalez, C., Jiménez, M. A., Rico, M., Santoro, J. & Nieto, J. L. (1992) *J. Am. Chem. Soc. 114*, 9676−9677.
Bruch, M. D., Dhingra, M. M., & Gierasch, L. M. (1991) *Proteins: Struct., Funct., Genet. 10*, 130−139.
Burgyone, R. D., & Geisow, M. J. (1989) *Cell Calcium 10*, 1−10.
Chaffotte, A. F., Cadieux, C., Guillou, Y., & Goldberg, M. E. (1992) *Biochemistry 31*, 4303−4308.
Darby, N. J., Morin, P. E., Talbo, G., & Creigton, T. E. (1995) *J. Mol. Biol. 249*, 463−477.
Dasgupta, S., & Bell, J. A. (1993) *Int. J. Pept. Protein Res. 41*, 499−511.
Dill, K. A. (1990) *Biochemistry 29*, 7133−7155.
Dobson, C. M. (1992) *Curr. Opin. Struct. Biol. 2*, 6−12.
Dobson, C. M., Evans, P. A., & Radford, S. E. (1994) *Trends Biochem. Sci. 19*, 31−37.
Dyson, H. J., & Wright, P. E. (1991) *Annu. Rev. Biophys. Biophys. Chem. 20*, 519−538.
Dyson, H. J., Rance, M., Houghten, R. A., Lerner, R. A., & Wright, P. E. (1988a) *J. Mol. Biol. 201*, 161−200.
Dyson, H. J., Rance, M., Houghten, R. A., Wright, P. E., & Lerner, R. A. (1988b) *J. Mol. Biol. 201*, 201−217.
Dyson, H. J., Merutka, G., Waltho, J. P., Lerner, R. A., & Wright, P. E. (1992a) *J. Mol. Biol. 226*, 795−817.
Dyson, H. J., Sayre, J. R., Merutka, G., Shin, H. C., Lerner, R. A., & Wright, P. E. (1992b) *J. Mol. Biol. 226*, 819−835.
Evans, P. A., Topping, K. D., Woolfsson, D. N., & Dobson, C. M. (1991) *Proteins: Struct., Funct., Genet. 9*, 248−266.
Gans, P. J., Lyu, P. C., Manning, M. C., Woody, R. W., & Kallenbach, N. R. (1991) *Biopolymers 31*, 1605−1614.
Garvey, E. P., Swank, J., & Matthews, C. R. (1989) *Proteins: Struct., Funct., Genet. 6*, 259−266.
Harper, E. T., & Rose, G. D. (1993) *Biochemistry 32*, 7605−7609.
Hooke, S. D., Radford, S. E., & Dobson, C. M. (1994) *Biochemistry 33*, 5867−5876.
Huber, R., Romisch, J., & Paques, E. P. (1990a) *EMBO J. 9*, 3867−3874.
Huber, R., Scheider, M., Myr, I., Romisch, J., & Paques, E. P. (1990b) *FEBS Lett. 275*, 15−21.

Huber, R., Berendes, R., Burger, A., Schneider, M., Karshikov, A., Luecke, H., Romisch, J., & Paques, E. P. (1992) *J. Mol. Biol. 223*, 683−704.
Huyghes-Despointes, B. M. P., Scholtz, J. M., & Baldwin, R. L. (1993) *Protein Sci. 2*, 80−85.
Jennings, P. A., & Wright, P. E. (1993) *Science 262*, 892−896.
Jiménez, M. A., Blanco, F. J., Rico, M., Santoro, J., Herranz, J., & Nieto, J. L. (1992) *Eur. J. Biochem. 207*, 39−49.
Jiménez, M. A., Muñoz V., Rico, M., & Serrano, L. (1994) *J. Mol. Biol. 242*, 487−496
Lyu, P. C., Gans, P. J., & Kallenbach, N. R. (1991) *J. Mol. Biol. 223*, 343−350.
Lyu, P. C., Wemmer, D. E., Zhou, H. X., Pinker, R. J., & Kallenbach, N. R. (1993) *Biochemistry* 32, 412−425.
Macquaire, F., Baleux, F., Huynh-Dinh, T., Neumann, J. M., & Sanson, A. (1992) *Int. J. Pept. Protein Res. 39*, 117−122.
Macquaire, F., Baleux, F., Huynh-Dinh, T., Rouge, D., Neumann, J. M., & Sanson, A. (1993) *Biochemistry 32*, 7244−7254.
Merrifield, R. B. (1963) *J. Am. Chem. Soc. 85*, 2149−2154.
Merutka, G., Dyson, H. J., & Wright, P. E. (1995) *J. Biomol. NMR 5*, 14−24.
Mitchell, J. B. O., Thornton, J. M., Singh, J., & Price, S. L. (1992) *J. Mol. Biol. 226*, 251−262.
Montelione, G. T., & Sheraga, H. A. (1989) *Acc. Chem. Res. 22*, 70−76.
Moss, S. E., Ed. (1992) *Annexins*, Portland Press, London.
Muñoz, V., & Serrano, L. (1994) *Nature: Struct. Biol. 1*, 399−409.
Muñoz, V., & Serrano, L. (1995) *J. Mol. Biol. 245*, 275−296.
Muñoz, V., Blanco, F. J., & Serrano, L. (1995) *Nature: Struct. Biol. 2*, 380−386.
Nandi, C. L., Singh, J., & Thornton, J. M. (1993) *Protein Eng. 3*, 6247−6259.
Neri, D., Billeter, M., Wider, G., & Wüthrich, K. (1992) *Science 257*, 1559−1563.
Pintar, A., Chollet, A., Bradshaw, C., Chaffotte, A., Cadieux, C., Rooman, M. J., Hallenga, K., Knowles, J., Goldberg, M., & Wodak, S. (1994) *Biochemistry 33*, 11158−11173.
Plateau, P., & Guéron, M. (1982) *J. Am. Chem. Soc. 104*, 7310−7311.
Presta, L. G., & Rose, G. D. (1988) *Science 240*, 1632−1641.
Raynal, P., & Pollard, H. B. (1994) *Biochim. Biophys. Acta 1197*, 63−93.
Richardson, J. S., & Richardson, D. C. (1988) *Science 240*, 1648−1652.
Romisch, J., & Paques, E. P. (1991) *Med. Microbiol. Immunol. 180*, 109−126.
Scholtz, J. M., & Baldwin, R. L. (19) *Annu. Rev. Biophys. Struct. 21*, 95−118.
Seale, J. W., Srinivasan, R., & Rose, G. D. (1994) *Protein Sci. 3*, 1741−1745.
Serrano, L., Sancho, J., Hirshberg, M., & Fersht, A. R. (1992) *J. Mol. Biol. 227*, 544−559.
Shaw, G. S., Hodges, R. S., Kay, C. M., & Sykes, B. D. (1994) *Protein Sci. 3*, 1010−1019.
Shin, H. C., Merutka, G., Waltho, J. P., Wright, P. E., & Dyson, H. J. (1993a) *Biochemistry 32*, 6348−6355.
Shin, H. C., Merutka, G., Waltho, J. P., Tennant, L. L., Dyson, H. J., & Wright, P. E. (1993b) *Biochemistry 32*, 6356−6364.
Shortle, D. (1993) *Curr. Opin. Struct. Biol. 3*, 66−74.
Smith, L. J., Alexandrescu, A. T., Pitkeathly, M., & Dobson, C. M. (1994) *Structure 2*, 703−712.
Sopkova, J., Renouard, M., & Lewit-Bentley, A. (1993) *J. Mol. Biol. 234*, 816−825.
Summers, M. F., South, T. L., Kim, B., & Hare, D. R. (1990) *Biochemistry 29*, 329−340.
Tam, J. P., & Heath, W. F. (1983) *J. Am. Chem. Soc. 105*, 6442−6447.
Taylor, W. R., & Geisow, M. J. (1987) *Protein Eng. 1*,183−187.
Waltho, J. P., Feher, V. A., Merutka, G., Dyson, H. J., & Wright, P. E. (1993) *Biochemistry 32*, 6337−6347.
Weng, X., Luecke, H., Song, I. S., Kang, D. S., Kim, S.-H., & Huber, R. (1993) *Protein Sci. 2, 448*−458.
Wishart, D. S., Sykes, B. D., & Richards, F. M. (1991) *J. Mol. Biol. 222*, 311−333.
Wishart, D. S., Sykes, B. D., & Richards, F. M. (1992) *Biochemistry 31*, 1647−1651.
Wray, V., Federeau, T., Gronwald, W., Mayer, H., Schomburg, D., Tegger, W., & Wingender, E. (1994) *Biochemistry 33*, 1684−1693.
Wright, P. E., Dyson, H. J., & Lerner, R. A. (1988) *Biochemistry 27*, 7167−7175.
Wüthrich, K. (1986) *NMR of Proteins and Nucleic Acids*, John Wiley and Sons, New York.
Zaima, H., Ueyama, N., Nakamura, A., & Aimoto, S. (1993) *Chem. Lett. 1993*, 1885−1888.
Zhang, O., & Forman-Kay, J. D. (1995) *Biochemistry 34*, 6784−6794.
Zhou, N. E., Kay, C. M., Sykes, B. D., & Hodges, R. S. (1993) *Biochemistry 32*, 6190−6197.

BI9509356